DINAME 2017 - Proceedings of the XVII International Symposium on Dynamic Problems of Mechanics
A. T. Fleury, D. A. Rade, P. R. G. Kurka (Editors), ABCM, São Sebastião, SP, Brazil, March 5-10, 2017

Operational modal analysis under wind load using stochastic subspace identification

Gustavo B. Wagner[1], **Damien Foiny**[1], **Rubens Sampaio**[1], **Roberta Lima**[1]

[1] Pontifícia Universidade Católica do Rio de Janeiro - Rua Marquês de São Vicente, 225, Gávea - Rio de Janeiro, RJ - Brasil - 22451-900 , gustavo_gbw@hotmail.com, damien.foiny@gmail.com, rsampaio@puc-rio.br, robertalima@puc-rio.br

Abstract: The extraction of modal parameters from a real structure represents an important step in modal analysis. When only the output signal is available in an experiment, the system identification process is referred as operation modal analysis (OMA). Applications of those cases are fond for structures where the ambient excitation (wind, traffic, waves, nearby systems, etc.) can not be removed or is the only possible one. Since the input signals can not be measured, some assumptions in their random nature are needed together with a stochastic modeling of the system. Among several methods, the stochastic subspace identification (SSI) has shown to be a consistent one and, therefore, was chosen to be used in this paper. Here, the modal analysis of a system under wind load is studied. The fluid-structure interaction force is usually not easy to be represented and its whiteness (assumption made in most of OMA methods) can not be easily conformed. Therefore, a two floor building model is used for an experimental validation, where different fluid-structure interactions were created. The paper begins with a presentation of the discrete state space model followed by the SSI theory. Two popular SSI algorithms are presented: covariance-driven and data-driven. A efficient way to correctly select the modal parameters is discussed together with a procedure to analyze the results. To exemplify the identification process, experimental results are shown and the identified parameters are listed. As conclusion, the wind has shown to be a good excitation source for OMA once the system has been correctly identified.

Keywords: Operational modal analysis, System identification, Stochastic subspace methods, wind excitation, experimental validation

INTRODUCTION

Operational Modal Analysis (OMA) consist in finding the dynamic characteristic of a structure through its modal parameters using output-only signals. Differently from the classical approach of Experimental Modal Analysis (EMA), where the input signal are also measured, OMA only uses the stochastic nature of the inputs, assumed to be random due the ambient conditions. This fact allows system identification to be done under circumstances where EMA is limited, which includes: large and heavy structures, where a controlled input is hard to apply and expensive, and identification of systems under operational conditions, where interferences from the location can not be eliminated.

With its majors developments happening in the early 1990s, applications of OMA in the structural dynamic field is far from reaching its total potential. Nowadays, OMA has been used as tool in two main areas. The first is in the model validation of large structures such as bridges, tall buildings, stadiums and oil rigs (Rainieri and Fabbrocino, 2014)(Rodrigues, 2004)(Brincker and Ventura, 2015). Those structures have in common the heavy weight and an acting ambient forces. The excitation sources can be the wind, traffic, and waves which are difficult to model and measure. Therefore, OMA methods for parameters estimations suits very well in those cases (Reynders *et al.*, 2016) (Reynders *et al.*,2008a). Recent articles have also focused on the variance estimation of the modal parameters. Mellinger *et al.* (2016), for example, measured the uncertainties in the modal parameter of an aircraft during in-flight tests. OMA has also been developed in the recent years for the field of structural health monitoring (SHM)(Liu, 2011)(Farrar and Worden, 2013)(Deraemacker and Worden, 2010). SHM is done by a periodic modal identification, which evaluates a possible change in the modal parameters. Cracks, corrosion, unfastened bolts, etc. usually reduces the system stiffness modifying natural frequencies and mode shapes.

The purpose of this article is to demonstrate a complete procedure for system identification of a real structure under wind load using stochastic subspace method. Becoming popular in the 2000s, stochastic subspace identification (SSI) consists in a collection of techniques that can be formulated in a consistent framework, where properties of the system can be estimated through a matrix subspaces. The two principal subspace algorithms found in the literature are the covariance-driven and the data-driven, which consist in estimating the system controllability matrix using covariance matrices or orthogonal projections of the output signals. For a clear understanding of such methods, the extension of the state space model are done by arranging the data in Hankel matrices. The method performance heavily depends in the Hankel matrices dimensions, and therefore are parameters that need to be carefully chosen.

The article starts with the vibration modeling of the system, where the discrete state space model is presented. With the application of a z-transform, it is possible to show how the modal parameters can be extracted from such model. After the definition of Hankel matrix, the state space formulation is extended to a better format for stochastic subspace identification. The two algorithms, covariance-driven and data-driven, are then demonstrated followed by their respective properties. To exemplify the methods, a real structure is tested to illustrate the identification procedure, which starts by finding the system order, estimating the observability matrix and extracting the modal parameters. The chosen model simulates a two-floor building, where the natural frequencies, damping factors and modes are identified under wind excitations. Different fluid-structure interaction tests are performed and demonstrate the method potential. An analysis of results are done by using a stabilization diagram, modal assurance criterion (MAC) and modal fitting of the correlation function.

DYNAMIC MODEL

A structure or mechanical system can, in most of the cases, be well represented by a discrete model such as

$$\mathbf{M}\ddot{\mathbf{q}}(t)+\mathbf{C}\dot{\mathbf{q}}(t)+\mathbf{K}\mathbf{q}(t)=\mathbf{B}_f\mathbf{u}(t), \tag{1}$$

where $\mathbf{M}$, $\mathbf{C}$ and $\mathbf{K}\in\mathbb{R}^{m\times m}$ are the inertia, damping and stiffness matrix respectively, and m is the number of degrees of freedom . The vector $\mathbf{q}(t)\in\mathbb{R}^{m\times 1}$ represents the displacements of the modal points, $\mathbf{B}_f\in\mathbb{R}^{m\times n_i}$ is a selection matrix for the force vector $\mathbf{u}(t)\in\mathbb{R}^{n_i\times 1}$ (select the degree of freedom where the forces are applied), and n_i is the number of knowing input acting in the system.

Considering that an experiment is performed and sensors are used to measure the system responses, the output observations signals can then be describe as

$$\mathbf{y}(t)=\mathbf{P}_a\ddot{\mathbf{q}}(t)+\mathbf{P}_v\dot{\mathbf{q}}(t)+\mathbf{P}_d\mathbf{q}(t), \tag{2}$$

where $\mathbf{y}(t)\in\mathbb{R}^{n_o\times 1}$ is the output signal vector and n_o is the number of output sensors. Matrices $\mathbf{P}_a$, $\mathbf{P}_v$ and $\mathbf{P}_d\in\mathbb{R}^{n_o\times n_o}$ are the influence matrices for acceleration, velocity and displacement, respectively.

Equations (1-2) are a second order differential equations that might be reduced to a so called state space model (Juang, 1994)

$$\dot{\mathbf{x}}(t) = \mathbf{A}_c\mathbf{x}(t)+\mathbf{B}_c\mathbf{u}(t) \tag{3}$$
$$\mathbf{y}(t) = \mathbf{P}\mathbf{x}(t)+\mathbf{D}\mathbf{u}(t) \tag{4}$$

where,

$$\mathbf{x}(t)=\begin{bmatrix}\mathbf{q}(t)\\ \dot{\mathbf{q}}(t)\end{bmatrix},\qquad \mathbf{A}_c=\begin{bmatrix}0 & \mathbf{I}\\ -\mathbf{M}^{-1}\mathbf{K} & -\mathbf{M}^{-1}\mathbf{C}\end{bmatrix},\qquad \mathbf{B}_c=\begin{bmatrix}0\\ \mathbf{M}^{-1}\mathbf{B}_f\end{bmatrix}.$$

$$\mathbf{C}=\begin{bmatrix}\mathbf{P}_d-\mathbf{P}_a\mathbf{M}^{-1}\mathbf{K} & \mathbf{P}_v-\mathbf{P}_a\mathbf{M}^{-1}\mathbf{C}\end{bmatrix},\qquad \mathbf{D}=\mathbf{P}_a\mathbf{M}^{-1}\mathbf{B}_f$$

The vector $\mathbf{x}(t)\in\mathbb{R}^{n\times 1}$ represents the states of the system, where $n=2m$ is the state space order and is the first parameter to be determined during the identification process. $\mathbf{A}_c\in\mathbb{R}^{n\times n}$ is called dynamic matrix and contains all informations about the modal parameters (natural frequencies, damping ratios and modes shapes).

Although the physical properties are continuous in time, a digitalization process always occurs during signal acquisition. This fact contributes to the choice of a discrete state space model. It can be obtain from Eq. (3-4) assuming a constant sample interval Δt and the hypotheses of zero-order hold for the input (constant values between samples). The continuous state space are then discretized as

$$\mathbf{x}(k+1) = \mathbf{A}\mathbf{x}(k)+\mathbf{B}\mathbf{u}(k) \tag{5}$$
$$\mathbf{y}(k) = \mathbf{P}\mathbf{x}(k)+\mathbf{D}\mathbf{u}(k). \tag{6}$$

for $k=1,2,\dots$, where

$$\mathbf{A}=e^{\mathbf{A}_c\Delta t},\qquad \mathbf{B}=\int_0^{\Delta t}e^{\mathbf{A}_c\tau'}d\tau'\mathbf{B}_c \tag{7}$$

Since in OMA the forces are unknown (unmeasured), some modification in Eq. (5-6) are needed. Letting $\mathbf{u}(k)=0$, the two white noise zero mean vectors (Cursi and Sampaio 2015) $\mathbf{w}(k)\in\mathbb{R}^{n\times 1}$ and $\mathbf{v}(k)\in\mathbb{R}^{n_o\times 1}$ are added into Eq. (5) and Eq. (6) respectively. The $\mathbf{w}(k)$ vector represents the ambient force (wind, waves, traffic, seismic waves, ground excitation) while $\mathbf{v}(k)$ represents the noise in the output sensors. Equations (5-6) are then modified into

$$\mathbf{x}(k+1) = \mathbf{A}\mathbf{x}(k)+\mathbf{w}(k) \tag{8}$$
$$\mathbf{y}(k) = \mathbf{P}\mathbf{x}(k)+\mathbf{v}(k). \tag{9}$$

with,

$$\mathbf{E}\left(\begin{bmatrix}\mathbf{w}(p)\\ \mathbf{v}(p)\end{bmatrix}\begin{bmatrix}\mathbf{w}(q) & \mathbf{v}(q)\end{bmatrix}\right)=\begin{bmatrix}\mathbf{Q} & \mathbf{S}\\ \mathbf{S}^T & \mathbf{R}\end{bmatrix}\delta_{pq}. \tag{10}$$

$\mathbf{E}(\square)$ is the expect value operator, while $\mathbf{Q}\in\mathbb{R}^{n\times n}$, $\mathbf{S}\in\mathbb{R}^{n\times n_o}$ and $\mathbf{R}\in\mathbb{R}^{n_o\times n_o}$ are the noises covariance matrices.

In order to obtain the poles of the system (a parameter that contains informations about the natural frequencies and damping ratios), the z-transform of both sides in Eq. (8-9) are performed, resulting in the parametrization of the transfer function

$$Y(z)=\mathbf{P}(z\mathbf{I}-\mathbf{A})^{-1}W(z)+V(z)=\mathbf{H}(z)W(z)+V(z)$$

Following Cramer's rule, one has (Deraemaeker and Worden, 2010)

$$(z\mathbf{I}-\mathbf{A})^{-1}=\frac{\text{adj}(z\mathbf{I}-\mathbf{A})}{\det(z\mathbf{I}-\mathbf{A})}, \tag{11}$$

where $\det(\square)$ represents the determinant and $\text{adj}(\square)$ the adjoint matrix. With Eq. (11), the poles of the transfer function are shown to be the eigenvalues of $\mathbf{A}$, since $\det(z\mathbf{I}-\mathbf{A})$ represents its characteristic polynomial.

Defining λ_i and ϕ_i as the eigenvalues and eigenvectors of $\mathbf{A}$, the modal parameter of the system can be obtain as (Brincker and Ventura, 2015)

$$\mu_i=\frac{\log(\lambda_i)}{\Delta t},\quad f_i=\frac{|\mu_i|}{2\pi},\quad \zeta_i=\frac{-\text{Re}(\mu_i)}{|\mu_i|},\quad \psi_i=\mathbf{P}\phi_i;\quad i=1,\ldots,n \tag{12}$$

where μ_i is the continuous poles, f_i the natural frequencies, ζ_i the damping ratios and ψ_i the mode shapes.

NOTATION

To a clear interpretation of the SSI method, the state space model defined by Eq. (8-9) is extended to a more convenient format. Therefore, some matrix notation need to be defined. Let a discrete signal $\mathbf{s}$ with N_s samples be given. Each signal sample are vector $\mathbf{s}_k\in\mathbb{R}^{r\times 1}$, which can be arranged in a Hankel matrix format as

$$\mathbf{S}_{i|j}\triangleq\begin{bmatrix}\mathbf{s}_i & \mathbf{s}_{i+1} & \cdots & \mathbf{s}_{i+N-1}\\ \mathbf{s}_{i+1} & \mathbf{s}_{i+2} & \cdots & \mathbf{s}_{i+N}\\ \vdots & \vdots & \ddots & \vdots\\ \mathbf{s}_j & \mathbf{s}_{j+1} & \cdots & \mathbf{s}_{j+N-1}\end{bmatrix}\in\mathbb{R}^{(j-i+1)r\times N},$$

where i and j are integer numbers, with $j>i$. Those subscripts in $S_{i|j}$ indicates the first and last time instant of the elements in the first column of the Hankel block matrix. Note that each element in the block matrix is a vector of dimension $r\times 1$. Since it is usually desired in SSI that all available vector samples are used, the relationship $j+N-1=N_s$ must be fulfilled. This means that if the number of block lines $(j-i)$ increases, the number of columns (N) automatically decreases.

Using the Hankel matrix format, one can arrange all systems signals, $\mathbf{y}(k)$, $\mathbf{w}(k)$ and $\mathbf{v}(k)$, and states $\mathbf{x}(k)$, as

$$\begin{aligned}\mathbf{Y}_p\triangleq\frac{1}{\sqrt{N}}\mathbf{Y}_{0|q-1},\quad \mathbf{Y}_f\triangleq\frac{1}{\sqrt{N}}\mathbf{Y}_{q|q+p-1},\quad \mathbf{W}_p\triangleq\frac{1}{\sqrt{N}}\mathbf{W}_{0|q-1},\quad \mathbf{W}_f\triangleq\frac{1}{\sqrt{N}}\mathbf{W}_{q|q+p-1},\\ \mathbf{V}_p\triangleq\frac{1}{\sqrt{N}}\mathbf{V}_{0|q-1},\quad \mathbf{V}_f\triangleq\frac{1}{\sqrt{N}}\mathbf{V}_{q|q+p-1},\quad \mathbf{X}_p\triangleq\frac{1}{\sqrt{N}}\mathbf{X}_{0|0},\quad \mathbf{X}_f\triangleq\frac{1}{\sqrt{N}}\mathbf{X}_{q|q}.\end{aligned} \tag{13}$$

The subscripts p and f in Eq. (13) stands for "past" and "future", and the integer number q (number of block lines) is an important parameter to be chosen as explained in the next section. Using Eq. (13), the discrete state space model, Eq. (8-9), can be extended to

$$\begin{aligned}\mathbf{Y}_p &= \Gamma_q\mathbf{X}_p+\mathbf{H}_q\mathbf{W}_p+\mathbf{V}_p\\ \mathbf{Y}_f &= \Gamma_q\mathbf{X}_f+\mathbf{H}_q\mathbf{W}_f+\mathbf{V}_f\\ \mathbf{X}_f &= \mathbf{A}^q\mathbf{X}_p+\Delta_q\mathbf{W}_p,\end{aligned} \tag{14}$$

where,

$$\Gamma_q=\begin{bmatrix}\mathbf{P}\\ \mathbf{PA}\\ \mathbf{PA}^2\\ \vdots\\ \mathbf{PA}^{q-1}\end{bmatrix},\quad \mathbf{H}_q=\begin{bmatrix}0 & 0 & 0 & \ldots & 0\\ \mathbf{P} & 0 & 0 & \ldots & 0\\ \mathbf{PA} & \mathbf{P} & 0 & \ldots & 0\\ \vdots & \vdots & \vdots & \ddots & \vdots\\ \mathbf{PA}^{q-2} & \mathbf{PA}^{q-3} & \mathbf{PA}^{q-4} & \ldots & 0\end{bmatrix},\quad \Delta_q=\begin{bmatrix}\mathbf{A}^{q-1} & \mathbf{A}^{q-2} & \ldots & \mathbf{A} & \mathbf{I}\end{bmatrix}. \tag{15}$$

Γ_q is the well known observability matrix of the system and Δ_q can be seen as the controllability matrix when $\mathbf{B}=\mathbf{I}$. The stochastic subspace identification method are based in the estimation of the observability matrix, in which the matrices $\mathbf{A}$ and $\mathbf{P}$ can be extracted and the modal parameters obtained by Eq. (12).

STOCHASTIC SUBSPACE IDENTIFICATION

The stochastic subspace identification method is presented here as in Mellinger *et al.* (2016), where three main steps are performed. In the literature, two SSI algorithms are often used: covariance-driven and data-driven. The differences between both consists only in the so called second step, where a matrix $\mathbf{O}_q$ is obtained with the calculations of covariance matrices or orthogonal projections. It is shown here that this matrix can be factorized into $\mathbf{O}_q = \Gamma_q \mathbf{Z}$, where the $\mathbf{Z}$ matrix depends on the algorithm used. The observability matrix can then be estimated as the column space of $\mathbf{O}_q$ after a singular value decomposition.

First Step - Hankel matrix

Since the only available signal in OMA is the system response, the method starts by building the $\mathbf{Y}_p$ and $\mathbf{Y}_f$ Hankel matrices. Therefore, the number of block lines q and the number of columns N need to be properly chosen. A right selection of the parameters will heavily contributes to the methods performance.

It is shown in the second and third steps that the maximum state space order that can be identified is $q \times n_o$. This means that the number of block lines q needs to be at least higher than n/n_o, to allow all modes to be identified. Since in a real case the true order n is unknown, it is recommended that q be large enough until at least mathematical (noise) modes can be found. This indicates that all physical modes have already been identified and the fact of increasing the system order will not bring new physical informations. This process can be well illustrated by a stabilization diagram as explained later.

Another concern with the number of block lines appears when a system has a low eigenfrequency compared with the sampling frequency. If q is a small number, only a part of the lower eigenperiods will be present in each column of $\mathbf{Y}_p$ and $\mathbf{Y}_f$. This fact decreases the quality in the identification. As proposed by Reynders and De Roeck (2008b), q can be chosen according to

$$q \geqslant \frac{f_s}{2f_0}, \tag{16}$$

where f_s is the sampling frequency and f_0 is the lowest frequency of interest. Since the number of output sensors in the test is often large, Eq. (16) usually satisfy also the order criteria mentioned first.

To define the number of columns N in the Hankel matrices, the singular value decomposition of $\mathbf{O}_q$ must be evaluated. In the second step, $\mathbf{O}_q$ is obtained through the estimated covariance matrices between $\mathbf{Y}_p$ and $\mathbf{Y}_f$. The true value of a covariance matrix is only obtained when $N \to \infty$, which means that N must be large enough until the singular values of $\mathbf{O}_q$ achieve a convergence. A good procedure to check if N is large enough consists in repeatedly calculates the singular values of $\mathbf{O}_q$ for different number of columns in $\mathbf{Y}_p$ and $\mathbf{Y}_f$. Figure 1 exemplifies this process, where in this case $N \geqslant 3 \times 10^4$ would be sufficient.

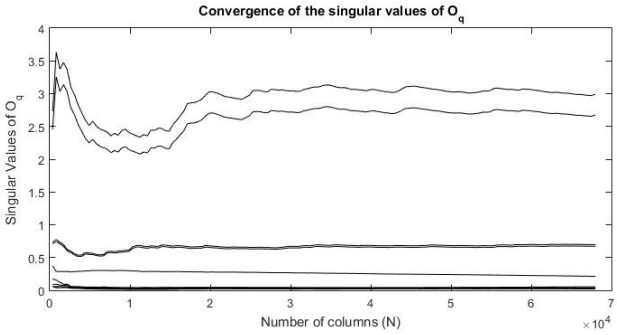

Figure 1 – Study of the singular values convergence of matrix $\mathbf{O}_q$.

Second Step - $\mathbf{O}_q$ matrix

This step of the SSI method consists in calculation of the so called $\mathbf{O}_q$ matrix. It can be done manipulating $\mathbf{Y}_p$ and $\mathbf{Y}_f$ Hankel matrices in different ways, depending on the chosen algorithm. The main idea is to form $\mathbf{O}_q$ as a product of $\Gamma_q \mathbf{Z}$ so the observability matrix can be estimated as its column space.

Before presenting the covariance-driven and data-driven algorithms, it is shown how to estimate the cross- and auto-covariance matrices of the system output signals. The estimate cross-covariance matrix of two arbitrary signals $\mathbf{a}$ and $\mathbf{b}$ with N available samples is define as

$$R_{[a,b]_\tau} = \frac{1}{N} \sum_{k=1}^{N} \mathbf{a}(k+\tau)\mathbf{b}^T(k), \tag{17}$$

where τ is the time lag between the signals. The auto-covariance matrices are estimated when $\mathbf{a} = \mathbf{b}$. When using the output "past" and "future" Hankel matrix, Eq. (13), the output auto-covariance matrices can be estimated in a practical

way through the products

$$\mathbf{Y}_f\mathbf{Y}_p^T = \begin{bmatrix} R_{[y,y]_q} & R_{[y,y]_{q-1}} & \cdots & R_{[y,y]_1} \\ R_{[y,y]_{q+1}} & R_{[y,y]_q} & \cdots & R_{[y,y]_2} \\ \vdots & \vdots & \ddots & \vdots \\ R_{[y,y]_{2q-1}} & R_{[y,y]_{2q-2}} & \cdots & R_{[y,y]_q} \end{bmatrix}, \tag{18}$$

and

$$\mathbf{Y}_p\mathbf{Y}_p^T = \mathbf{Y}_f\mathbf{Y}_f^T = \begin{bmatrix} R_{[y,y]_0} & R_{[y,y]_{-1}} & \cdots & R_{[y,y]_{1-q}} \\ R_{[y,y]_1} & R_{[y,y]_0} & \cdots & R_{[y,y]_{2-q}} \\ \vdots & \vdots & \ddots & \vdots \\ R_{[y,y]_{q-1}} & R_{[y,y]_{q-2}} & \cdots & R_{[y,y]_0} \end{bmatrix}. \tag{19}$$

Equations (17) and (18) are block Toeplitz matrices, where each block is a estimated auto-covariance matrix using N (number of columns in the Hankel matrices) samples. This fact emphasizes the importance of a correct choice of the N columns in the first step.

Important assumptions are made in the following algorithms. The unknown inputs $\mathbf{w}(k)$ are assumed to be white noise processes, and the past outputs are assumed to be uncorrelated with the future unknown inputs and sensors noises. This means that both products, $\mathbf{W}_f\mathbf{Y}_p^T$ and $\mathbf{V}_f\mathbf{Y}p^T$, are equal to zero.

Covariance-driven

This algorithm is based on the estimated auto-covariance matrices in Eq. (18) and in the stochastic realization algorithm demonstrated by Deraemaeker and Worden (2010). Using Eq.(14), the $\mathbf{O}_{q\_cov}$ matrix can be define as

$$\begin{aligned} \mathbf{O}_{q\_cov} &\triangleq \mathbf{Y}_f\mathbf{Y}_p^T \\ &= \left(\Gamma_q\mathbf{X}_f + H_q\mathbf{W}_f + \mathbf{V}_f\right)\mathbf{Y}_p^T \\ &= \Gamma_q\mathbf{X}_f\mathbf{Y}_p^T \\ &= \Gamma_q\mathbf{Z}_{cov}. \end{aligned} \tag{20}$$

Through the stochastic realization algorithm, it can be shown that $\mathbf{Z}_{cov}$ is equal to the stochastic observability matrix.

Data-driven

This algorithm, also known as unweighted principal component, uses orthogonal projections of the row space of the "future" output Hankel matrix into the row space of the "past" output Hankel matrix. The matrix $\mathbf{O}_{q\_cov}$ can then be define as

$$\begin{aligned} \mathbf{O}_{q\_data} &\triangleq \text{Proj}_{\mathbf{Y}_p}\left(\mathbf{Y}_f\right) \\ &= \mathbf{Y}_f\mathbf{Y}_p^T\left(\mathbf{Y}_p\mathbf{Y}_p^T\right)^\dagger\mathbf{Y}_p \\ &= \Gamma_q\mathbf{Z}_{cov}\left(\mathbf{Y}_p\mathbf{Y}_p^T\right)^\dagger\mathbf{Y}_p \\ &= \Gamma_q\mathbf{Z}_{data}. \end{aligned} \tag{21}$$

In Overschee and De Moor (1996), $\mathbf{Z}_{data}$ is shown to be a sequence of Kalman filter states. It is also demonstrated that after a post multiplication of Eq. (21) by a weighted matrix, the data-driven algorithm leads to the same results of the covariance-driven. The orthogonal projection as demonstrated in Eq. (21) is not a computational efficient one. This problem can be overcome using a *QR*-factorization as shown in Overschee and De Moor (1996).

In both algorithms, the size of $\mathbf{O}_q$ is $qn_o \times qn_o$, which means that the maximum amount of singular values in a singular value decomposition is qn_o. As shown in the next section, this number is also the maximum state space order that can be identified.

Third Step - Modal parameters extraction

Independently of the the chosen algorithm, $\mathbf{O}_q$ has an important factorization property. Overschee and De Moor (1996) proves that $\mathbf{O}_q$ and Γ_q have the same column space. Assuming that the system is completely observable, Γ_q is expect to be of full rank and equal to n. For this reason, after a singular value decomposition (SVD) only n nonzero singular values are likely to be obtained. Since in real cases noises are always present in the signal, this number may be larger. It is up to the user to decide which singular values are related to physical modes and which are numerical modes. The best tool for this analysis is the stabilization diagram as presented in the next section.

Assuming that the matrix $\mathbf{O}_q$ has been correctly obtained, the SVD can be written, in the reduced form, as

$$\mathbf{O}_q = \begin{bmatrix}\mathbf{U}_1 & \mathbf{U}_2\end{bmatrix}\begin{bmatrix}\mathbf{S}_1 & 0 \\ 0 & 0\end{bmatrix}\begin{bmatrix}\mathbf{V}_1^T \\ \mathbf{V}_2^t\end{bmatrix} = \mathbf{U}_1\mathbf{S}_1\mathbf{V}_1^T. \tag{22}$$

An estimation of the observability can then be done as

$$\hat{\Gamma}_q = \mathbf{U}_1 \mathbf{S}_1^{\frac{1}{2}}. \tag{23}$$

Using Eq. (15), the output matrix $\mathbf{P}$ can be identified in a straightforward way as the first block row of $\hat{\Gamma}_q$. The dynamic matrix $\mathbf{A}$ is obtained in a least square sense. Defining, $\overline{\Gamma}_q$ and $\underline{\Gamma}_q$ as the matrix $\hat{\Gamma}_q$ without the first and last block rows, one has

$$\overline{\Gamma}_q = \begin{bmatrix} \mathbf{PA} \\ \vdots \\ \mathbf{PA}^{q-1} \end{bmatrix}, \qquad \underline{\Gamma}_q = \begin{bmatrix} \mathbf{P} \\ \vdots \\ \mathbf{PA}^{q-2} \end{bmatrix}. \tag{24}$$

The matrix $\mathbf{A}$ is then obtained as

$$\mathbf{A} = \underline{\Gamma}_q^{\dagger} \overline{\Gamma}_q \tag{25}$$

Once the state space matrices has been identified, the modal parameters can be extracted using Eq. (12).

RESULTS ANALYSIS

After a correct implementation of the method, a carefully interpretation of the results must be made. Since the true order of the system is unknown, it is a common practice to identify the modal parameters several times for an increasing number of model order. This process can be easily done by truncating the SVD in Eq. (22) for a increasing number of singular values each time. As a result, when n is higher than the real order, noise modes are also identified and modeled. However, their respective modal parameters are inconsistent and change their values for each order number. This means that the unstable parameters are most likely to be linked to noise modes while the stable ones are related to the true system. This characteristic is easily observed with a stabilization diagram as showed in Fig. 4. Following this procedure, even weakly excited system modes, that appear only when the models order is high, can be identify. Weakly excited modes are related to small singular values and therefore can be interpreted as noise modes at first, but not after checking their respective stability.

In the stochastic subspace identification theory it is assumed that the unknown inputs are white. However, in real life it is most likely to have colored noises instead. This fact may contribute to the appearance of stable modes but not related to the system. In those cases an evaluation of the parameters values shall be made, discarding for example cases where the damping is to high for the structure or the mode shapes are unrealistic.

For the SSI method, a good way to validate the identified results is trough a direct comparison between the autocorrelation function obtained by the data and the autocorrelation function obtained by the modal parameters. In Bricker and Ventura(2015) it is show how the output autocorrelation function can be expressed by the modal parameters. Figure 7 illustrates this validation procedure.

When performing OMA, a good practice is to use also another identification methods. In the literature, one can find several methods in time and frequency domains. Some of those methods can sometimes lead to a better result depending on the application and quality of the signal. A comparison between experimental and the numerical results should also be done when possible. A common tool for these purpose is the modal assurance criterion (MAC). When the same mode is identify by different methods, lets say $\mathbf{a}$ and $\mathbf{b}$, the MAC between them is calculated by

$$\mathrm{MAC}(\mathbf{a},\mathbf{b}) = \frac{|\mathbf{a}^H \mathbf{b}|^2}{(\mathbf{a}^H \mathbf{a})(\mathbf{b}^H \mathbf{b})}, \tag{26}$$

where $\square^H$ stands for complex conjugate transpose. If the estimated modes are similar, the MAC value is close to one.

EXPERIMENTAL ANALYSIS FOR WIND EXCITATION

The goal in this article is to show how the stochastic subspace technique can be used to perform an operational modal analysis of a structure under wind load. The wind force acting in a structure can not be measured with accuracy, leaving an output-only analysis the only possible choice. In the structural engineering field this kind of excitation must be considered in many application, for example, in tall buildings, bridges, antennas, etc. In those cases, the interaction between wind and structure is considered to be random.

The structure used here illustrates the case of a two-floor building model, as showed in Fig. 2a (Fonseca *et al.*, 2014). Two displacement laser sensors were used to collect the data from each floor in an unidimensional direction. A powerful wind blower has been put aside the structure to produce a wind with approximately constant speed. Two types of wind interaction has been proposed and illustrated by drawings in Fig. 2b and 2c. In the fist one, a plastic sheet was fixed in the structure to simulate a barrier caused by a wall and will be referred here as Test 1. The force in this case is assumed to be random and continuously distributed through the structure. In the second case, two small parachutes were fixed in each of the floors and will be referred here as Test 2. The interaction forces in this case is assumed to be random and concentrated

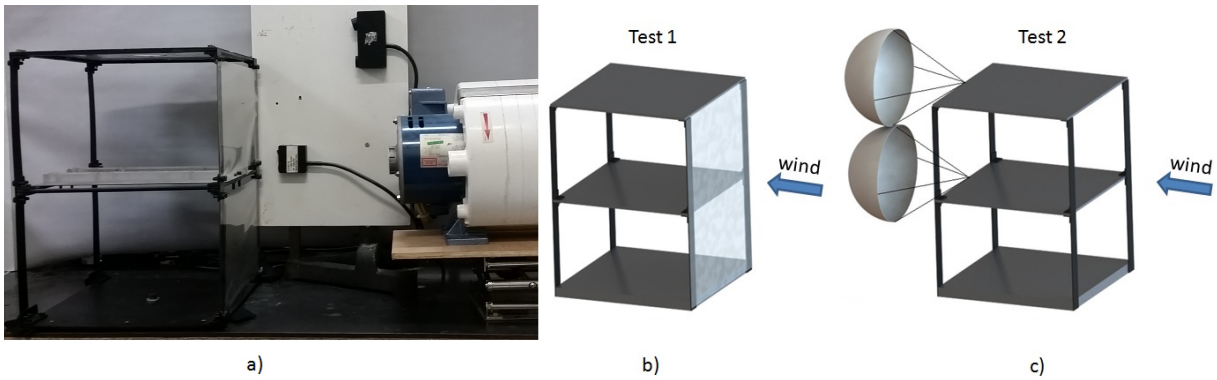

Figure 2 – a) Structure of the two floor building model. b) Respresentation of the wind interection force during the Test 1. c) Respresentation of the wind interection force during the Test 2.

in each floor. The intention of those barriers was to intensify the interaction forces in different ways without adding mass or stiffness in the structure.

When planing an experiment, the frequency band should always be the first parameter to be defined. This process is usually done with some a priori knowledge of the structure, as for example with a numerical simulation. For the two floor building model it was define that the frequency band was between 2 and 15 Hz. As consequence, the sampling frequency was chosen to be 150 Hz, leading to a desired oversampling factor of 10. Using the step 1 criteria, the number of block lines in the Hankel matrices should be $q = \frac{150}{2} = 75$. The number of samples N_s to be acquire depends on the convergence of $\mathbf{O}_q$ singular values. The convergence results of both tests are shown in Fig. 3. For Test 1 (Fig. 3a and 3b) it is possible to see that approximately only 4 singular values are different from zero, giving a first impression that the system order is $n = 4$. One should also note that those 4 singular values converge quickly to their respectively values. Now, for the Test 2 (Fig. 3c and 3d), it is possible to see the presence of 5 singular values, given the impression that $n = 5$. But, since state space order n is twice the dynamic system order m, having a odd number for n is a indicative that noise modes may be present in the data. In Fig. 3d it is possible to see that 4 of the 5 singular values converge to values different than zero, while the "noise" singular value decays toward zero. For both tests a value of $N_s = 10 \times 10^4$ is enough.

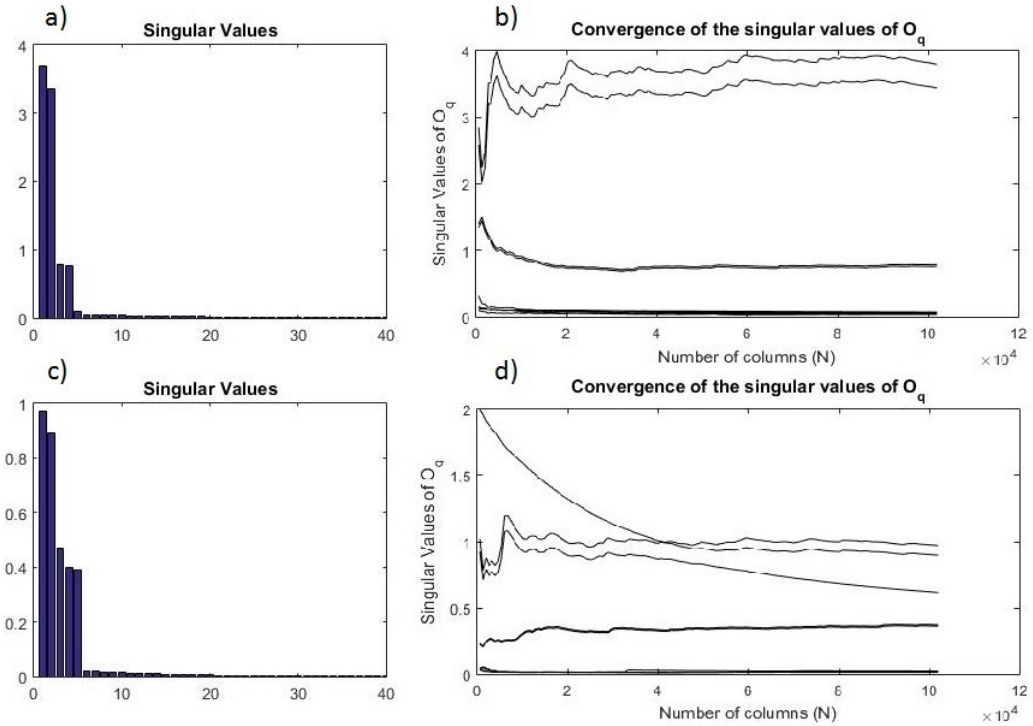

Figure 3 – a) Singular values for Test 1 with N = 102300 . b) Convergence of singular values for Test 1. c) Singular values for Test 2 with N = 102300 . d)Convergence of singular values for Test 2.

To find out the true order of the system, four stabilization diagrams were constructed as showed in Fig. 4. The possible values for n were chosen between 1 and 40. The identified natural frequencies with $\zeta_i < 1$ were marked in the diagram. The power spectral density of the output signals were also ploted in the same figure to a easy comparison between the marked natural frequency and the spectra peaks. All four charts have two spectra peaks coinciding with two stable natural frequency, leading to a conclusion that the true number of modes is 2. Comparing the Fig. 4a and 4b with Fig. 4c and

4d, one can see that the Test 1 has a clear stabilization diagram. There are almost no difference between the results from covariance-driven and data-driven algorithms.

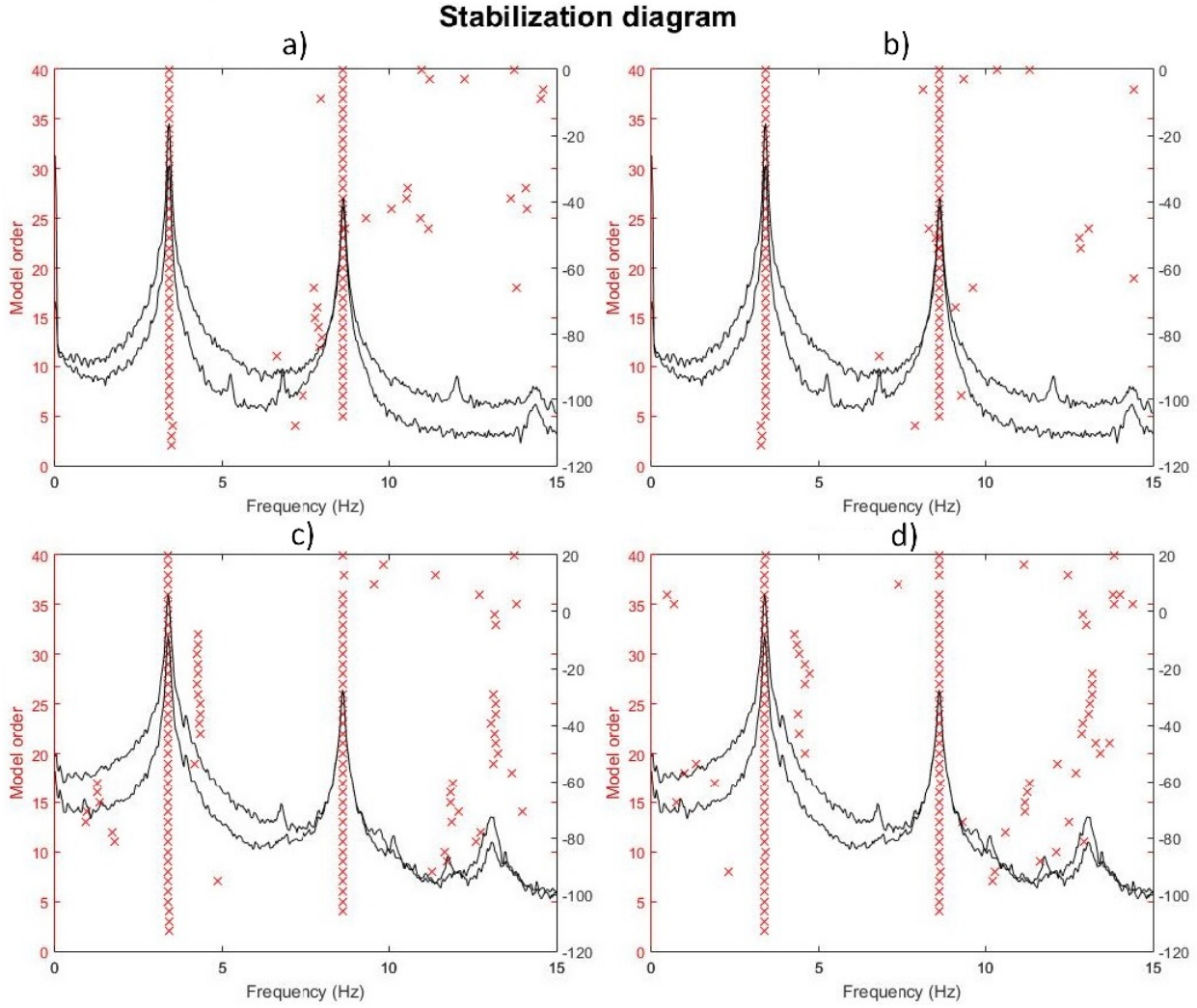

Figure 4 – Stabilization diagram for a) covariance-driven algorithm in Test 1. b) data-driven algorithm in Test 1. c) covariance-driven algorithm in Test 2. d)data-driven algorithm in Test 2.

The identified modal parameters for Tests 1 and 2 are listed in Tab. 1 and Tab. 2, respectively. Other identification methods were also applied to the same data to conform that the modal parameters were correctly identified. As one can see, the natural frequencies values for all methods were approximately the same while the damping factors had small differences. Damping evaluation can be very sensitive, making the identification process for the true value a hard task. Nevertheless, these differences found here do not significantly influence the dynamic behavior of the system, since their values are very small (less than 1%). It is possible to see that the damping ratios in Test 2 are, in most of the cases, higher than in Test 1. A explanation may be the air friction in the small parachutes that increase the damping. The natural frequencies in the other hand did not change their values, since the parachutes are very light and do not increase the stiffness between floors.

Table 1 – Identified modal prameters for Test 1.

Test 1	**Natural Frequency [Hz] (1º / 2º mode)**	**Damping Factor [%] (1º / 2º mode)**
SSI/Covariance-driven	3.40 / 8.63	0.65 / 0.41
SSI/Data-driven	3.39 / 8.63	0.72 / 0.44
ERA(1)	3.39 / 8.63	0.60 / 0.44
ITD(2)	3.39 / 8.62	0.25 / 0.55
ARPR(3)	3.39 / 8.61	0.71 / 0.67

(1) Eigensystem Realization Algorithm / (2) Ibrahim Time Domain / (3) AR model Poly Reference

To evaluate the quality of identified modes, a MAC between all tests and methods was perform and the results are showed in Fig. 5. The SSI data-driven were chosen arbitrarily as the reference result. The MAC between ARPR and SSI

Table 2 – Identified modal prameters for Test 2.

Test 2	Natural Frequency [Hz] (1º / 2º mode)	Damping Factor [%] (1º / 2º mode)
SSI/Covariance-driven	3.38 / 8.62	1.03 / 0.48
SSI/Data-driven	3.38 / 8.61	1.07 / 0.72
ERA(1)	3.38 / 8.62	0.94 / 0.47
ITD(2)	3.38 / 8.61	0.37 / 0.51
ARPR(3)	3.38 / 8.61	0.94 / 0.55

(1) Eigensystem Realization Algorithm / (2) Ibrahim Time Domain / (3) AR model Poly Reference

data-driven was the only one in which the modes did not perfectly agreed. The modes shapes for the SSI data-driven are drawn in Fig. 6 and were considered to be with realistic shapes.

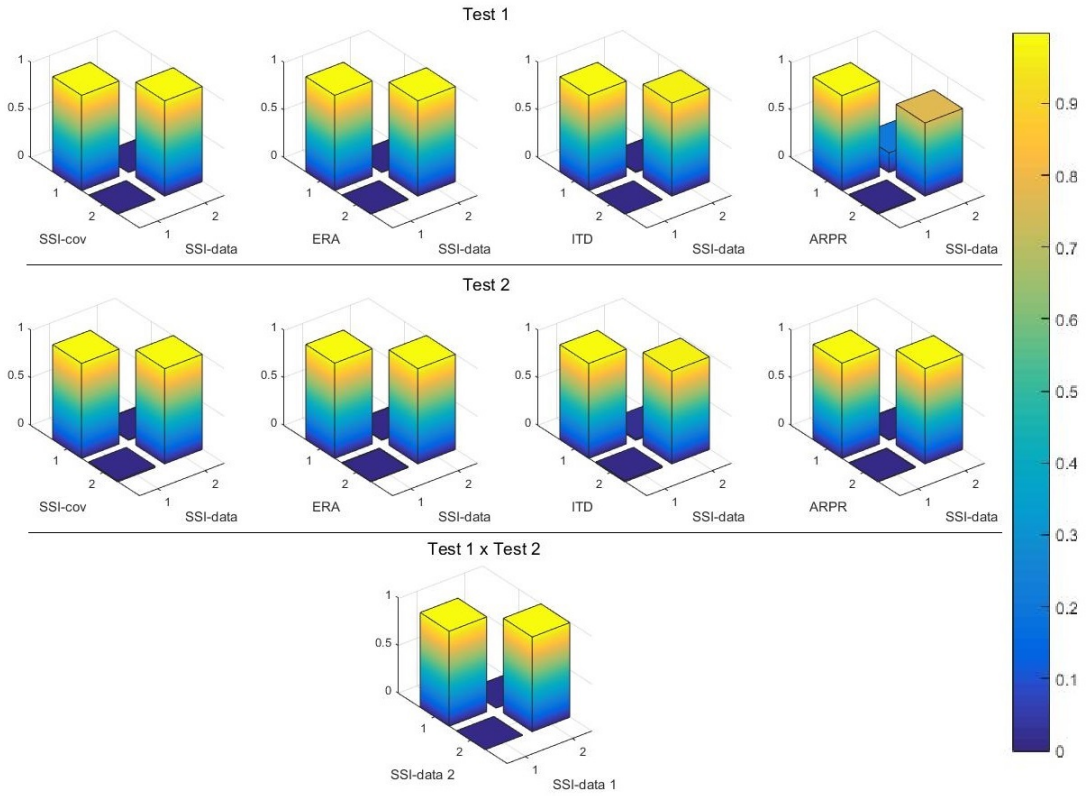

Figure 5 – Modal assurance criterion between methods and tests.

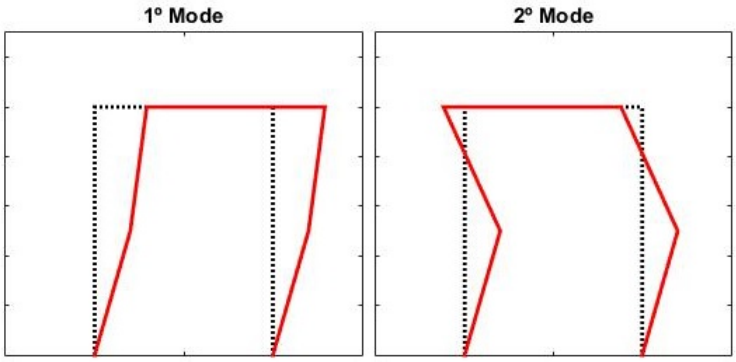

Figure 6 – Identified mode shapes

The last and probably the most important validation process is to create a autocorrelation function of the output signal in terms of the identified modal parameters. An analytical expression for such function can be found in Brincker and Ventura (2015). When the autocorrelation function of the measured output leads to a similar result, it is possible to say that the identified modal parameter are corrected identified. To exemplify this validation, the autocorrelation of the first floor was compared in Fig. 7 using the Test 1 data.

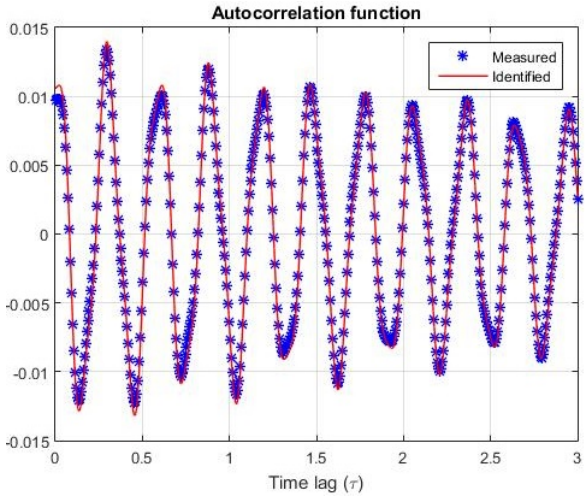

Figure 7 – Modal parameters validation trough autocorrelation of the first floor output signal

CONCLUSION

In this article, wind excitation were investigated as a possible random input for operational modal analysis. Different fluid-structure iterations have been created experimentally to observe if the hypotheses of randomness and frequency band excitation criteria were fulfilled. The results have shown a correct estimation of the modal parameters, together with the excitation of all interested modes. The stochastic subspace identification method has shown to be a powerful algorithm for OMA in systems with wind excitation. As conclusion, the method can be seen as a good choice for application in structure health monitoring of tall buildings, bridges and wind turbines.

REFERENCES

Brincker, R. and Ventura, C., 2015, "Introduction to operational modal analysis", John Wiley & Sons, West Sussex, UK.

Daraemaeker, A., Worden, K.(eds.), 2010, "New Trends in Vibration Based Structural Health Monitoring", CISM, Udine.

Farrar, C.R. and Worden, K., 2013, "Structural health monitoring: a machine learning perspective", John Wiley & Sons, West Sussex, UK.

Fonseca, C., Lima, R., Wagner, G. and Sampaio, R., 2014, "Design of a nonlinear dynamical absorber foran uncertain system", Proceedings of Uncertainties 2014, Rouen, France.

Juang, J., 1994, "Applied System Identification", Prentice Hall, Englewood Cliffs, NJ.

Liu. Y, 2011, "Bridge Health Monitoring, Maintenance and Safety", Trans Tech Publications, Switzerland, doi:10.4028/www.scientific.net/KEM.456.1

Mellinger, P., Döhlerm M. and Mevel, L., 2016, "Variance estimation of modal parameters from output-only and input/output subspace-based system identification", Journal of Sound and Vibration, Vol. 379, pp. 1-27, `http://dx.doi.org/10.1016/j.jsv.2016.05.037`

Overschee, P.V. and De Moor, B., 1996, "Subspace identification for linear systems", Kluwer Academic Publishers, Leuven.

Rainieri, C. and Fabbrocino, G., 2014, "Operational Modal Analysis of Civil Engineering Structures", Springer, New York.

Reynders, E., Maes, K., Lombaert, G. and De Roeck, G.,2016, "Uncertainty quantification in operational modal analysis with stochastic subspace identification: validation and application", Mechanical Systems & Signal Processing, Vol. 66-67, pp. 13-30, 2016. `http://dx.doi.org/10.1016/j.ymssp.2015.04.018`

Reynders, E., Pintelon, R. and De Roeck, G., 2008a, "Uncertainty bounds on modal parameters obtained from stochastic subspace identification", Mechanical Systems and Signal Processing, Vol. 22, pp. 948-969, doi:10.1016/j.ymssp.2007.10.009

Reynders, E. and De Roeck, G., 2008b, "Reference-based combined deterministic-stochastic subspace identification for experimental and operational modal analysis", Mechanical Systems and Signal Processing, Vol. 22, pp. 617-637, doi: 10.1016/j.ymssp.2007.09.004

Rodrigues, J., 2004, "Identificação Modal Estocástica", PhD theses, Universidade do Porto, Portugal.

Cursi, E.S. and Sampaio, R., 2015, "Uncertainty Quantiffication and Stochastic Modeling with Matlab", Elsevier, ISTE Press, UK, 442 p.

RESPONSIBILITY NOTICE

The authors are the only responsible for the material included in this paper.